



Axial multipoint laser Doppler velocimetry based on grating guidance

Qiuyuan Yu^{1,2} · Bohan Liu⁴ · Zhenhua Cong^{1,2,3} · Zhaojun Liu^{1,2,3} · Xiao Zhang^{5,6} · Luoyuan Qu⁷ · Shaojie Men^{1,2,3}

Received: 29 April 2024 / Accepted: 21 June 2024 / Published online: 26 June 2024
© The Author(s), under exclusive licence to Springer-Verlag GmbH Germany, part of Springer Nature 2024

Abstract

Laser Doppler velocimetry (LDV) technology is highly favored in the field of speed measurement for its high accuracy and resolution. However, it has limitations in specific applications due to its single-point speed measurement capability. To address this issue, a method of axial multi-point laser Doppler velocimetry is proposed to expand the application range of this technology. This method is based on the dual-beam laser Doppler velocimetry mode, utilizing the diffraction characteristics of the reflected grating to achieve spatial separation of measurement points axially. To verify the feasibility of the method, a laser Doppler velocimetry system was constructed, enabling velocity measurements at three axial points within a range of 0–14 m/s, with an average measurement error of less than 4%. Measurements of water flow velocity in a water tank pipeline were conducted, and compared with a standard electronic flowmeter, resulting in an average relative error of approximately 0.77%.

1 Introduction

Laser Doppler Velocimetry (LDV) is a non-contact, high-accuracy velocity measurement technique that allows fast response and high spatial resolution [1]. LDV is based on the Doppler effect and the interference principle of lasers and determines the velocity by analyzing the Doppler shift produced by the scattered light of moving particles. With advances in lasers, materials science, and computing, LDVs have evolved from early large-scale systems to today's portable devices, which have been successfully applied in the fields of fluid dynamics [2, 3], aerodynamics [4, 5],

biomedicine [6, 7], industrial inspection [8, 9] and traffic management [10, 11].

Although LDV can provide high-precision velocity measurements, traditional LDV systems are limited to single-point measurements, making it difficult to fully characterize complex and unsteady flow phenomena. For small-scale flow features, turbulence, boundary layers, flow instabilities, etc., there is a need for LDV systems capable of multi-point measurements to capture subtle variations in the flow field. Generating multiple measurement volumes using beam-splitting techniques is an effective approach, such as generating spatially separated beams with different frequencies through acousto-optic devices [12, 13], or focusing different wavelengths of light at

✉ Shaojie Men
shaojiemen@sdu.edu.cn

Qiuyuan Yu
202212638@mail.sdu.edu.cn

Bohan Liu
liu_bh@163.com

Zhenhua Cong
congzhenhua@sdu.edu.cn

Zhaojun Liu
zhaojunliu@sdu.edu.cn

Xiao Zhang
sdzhangxiao@sdu.edu.cn

Luoyuan Qu
549541464@qq.com

¹ School of Information Science and Engineering, Shandong University, Qingdao 266237, China

² Key Laboratory of Laser and Infrared Systems, Ministry of Education, Qingdao 266237, China

³ Key Laboratory of Laser Technology and Application, Qingdao 266237, China

⁴ China Ship Scientific Research Center, Wuxi 214000, China

⁵ Weifang Hydrodynamics Science and Technology Industry Institute, Weifang 261200, China

⁶ Laoshan Laboratory, Qingdao 266200, China

⁷ Shandong Guoyao Quantum Lidar Technology Co., Ltd., Jinan 250101, China

different focal points using an array of waveguide gratings in a fiber-optic configuration [14, 15]. Fu et al. [16] utilized an acoustic-optic modulator to introduce an optical frequency shift, thereby spatially encoding the measurement points and enabling accurate measurement of multipoint velocities with a single photodetector. In a recent study, Kyoden et al. [17] demonstrated a large-scale cross-sectional multipoint LDV that utilizes a two-dimensional fiber array to collect interferometric signals and is capable of measuring the velocity of multiple points on a cross-section within the overlapping region of two laser sheets over a measurement area of more than $150 \text{ mm} \times 10 \text{ mm}$.

Still, another way to realize multipoint velocity measurements is scanning LDV [18–20], which is capable of measuring the spatial distribution of velocity point by point by changing the position of the measurement points by mechanical or non-mechanical means. Mura et al. [21] worked on a non-mechanical scanning LDV, based on a grating and wavelength tuning technique to change the position of the measurement points in conjunction with a one-dimensional spatial encoding, demonstrating a compact differential laser Doppler velocimetry probe that measured a two-dimensional velocity distribution in the cross-section. In a recent study, they further extended the distribution measurement of velocity to three dimensions with a measurement error of 2.8–4.8% [22]. The method of scanning the measurement points by changing the wavelength facilitates the miniaturized design of the probe since no moving mechanism is required. However, the configuration and control of utilizing LiNO_3 frequency shifter arrays to generate spatial light separation is relatively complex, and the high cost of the devices is also a factor to be considered.

In this study, a method for generating axial multipoint LDVs based on a reflection grating guiding an incident laser is proposed. The method utilizes the multi-stage diffraction of the reflection grating to spatially divide the laser into multiple channels and acquire the Doppler shift based on the dual-beam mode. This design avoids complex optical system tuning and enables highly integrated and miniaturized velocity distribution measurements. To demonstrate the proposed method, a three-channel LDV experimental setup is built in this paper, and a rotating disk experiment and a water velocity measurement experiment are designed to test the performance of the setup.

2 Measurement principles and method design

2.1 Measurement principles and design

The schematic diagram of the proposed axial multipoint laser Doppler velocimetry system is shown in Fig. 1. The laser emits

a beam of light that is collimated by a collimating lens and then divided into two equal paths by a beam splitter. These two paths are incident on identical reflective gratings to form a multilevel diffracted light. The two beams with the same diffraction level intersect to create a measurement point in space. When a moving object passes through these measurement points, two beams of scattered light are converged by the receiving system onto the surface of the photodetector, generating a beat-frequency signal; the multi-stage diffraction of the reflective grating permits each stage of diffraction to be equivalent to an independent two-beam mode laser Doppler velocimetry system, enabling multi-point velocity measurements.

According to the principle of two-beam Doppler velocimetry [23], the Doppler frequency f_{Dm} of the m th diffracted light is related to the velocity of the object as shown in Eq. (1).

$$f_{Dm} = \frac{v_{m\perp} \cdot 2 \cdot \sin \frac{\theta_m}{2}}{\lambda} \quad (1)$$

The angle between the m th level of diffracted light illuminating an object is denoted by θ_m . The velocity component that is perpendicular to the two laser beams is denoted by $v_{m\perp}$. Equation (1) indicates that the Doppler frequency of the m th diffracted light is directly proportional to the velocity component $v_{m\perp}$ of the object's motion. By measuring the Doppler frequency, we can determine the velocity component of the object as it passes through the measurement region of the m th diffracted light as follows:

$$v_{m\perp} = \frac{f_{Dm} \lambda}{2 \sin \frac{\theta_m}{2}} \quad (2)$$

According to the equation of reflection grating, the relationship among the incidence angle α , diffraction angle γ_m , and grating constant d can be expressed as follows:

$$d(\sin \gamma_m + \sin \alpha) = \pm m \lambda. \quad (3)$$

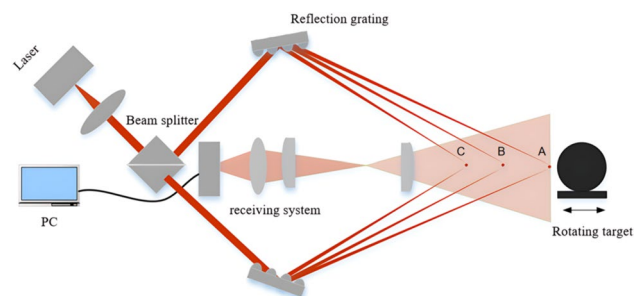


Fig. 1 Schematic diagram of the principle of axial multi-point laser Doppler velocimetry system

The diffraction angle of the m th diffracted light is as follows:

$$\gamma_m = \sin^{-1}\left(\frac{\pm m\lambda}{d} - \sin\alpha\right). \tag{4}$$

Based on the geometrical relationship depicted in Fig. 2, we can calculate the distance D_L between two adjacent measurement points along the axial direction as follows:

$$D_L = \frac{L}{2}(\tan(\gamma_{m+1} + \beta) - \tan(\gamma_m + \beta)). \tag{5}$$

where D_L represents the distance between two neighboring measurement points, β is the angle between the grating normal and the line connecting the two gratings, γ_m and γ_{m+1} correspond to the diffraction angle of the m th and $(m + 1)$ th level, respectively, and L is the distance between the two gratings. The overall measurement area range is determined by the number of measurement points and the distance between neighboring measurement points.

2.2 Testing system uncertainty models

To provide more parameters for better performance evaluation and result analysis of the proposed LDV velocimetry method. The modeling of the uncertainty of the proposed LDV velocimetry method is completed by following the GUM (Guide for the Expression of Uncertainty in Measurement) [24]. In order to avoid overemphasizing this part of the analysis, we chose to apply Eq. (1), limiting the uncertainty analysis to the output variable of the measured LDV speed.

By analyzing the parameters of Eq. 1, the parameters that mainly affect the output measurement speed are the laser wavelength, the Doppler shift, and the half angle of

the beam of the corresponding level. The following is an analysis of the corresponding uncertainties of these three parameters:

Assuming that the linewidth of the wavelength is u_1 , the actual laser output wavelength is $\lambda \pm u_1$;

The angle between the m th energy levels of the diffracted light illuminating the object was measured in the experiment using similar triangles, and if the uncertainty of the angle is, then the actual angle measured is $\theta \pm u_2$. Rules based on uncertainty propagation, if the uncertainty of is, then we can compensate for this uncertainty by adjusting the angle, and the angle should be adjusted with an accuracy of at least.

Assuming that the uncertainty of the Doppler shift is u_3 , the actual peak extraction of the Doppler shift is $f_{Dm} \pm u_3$;

Then, according to Eq. (1), the synthesized uncertainty is: According to the rule of uncertainty propagation, when the function v is a function of variable x_i , the synthetic uncertainty u_v is:

$$u_v = \sqrt{\left(\frac{\partial v}{\partial \lambda}u_1\right)^2 + \left(\frac{\partial v}{\partial \theta}u_2\right)^2 + \left(\frac{\partial v}{\partial f_d}u_3\right)^2}.$$

$$u_v = \sqrt{\left(\frac{f_{Dm}}{2\sin\frac{\theta_m}{2}}u_1\right)^2 + \left(\frac{\lambda f_{Dm} \cos\frac{\theta_m}{2}}{4\left(\sin\frac{\theta_m}{2}\right)^2}u_2\right)^2 + \left(\frac{\lambda}{2\sin\frac{\theta_m}{2}}u_3\right)^2}. \tag{6}$$

From this we have modeled the uncertainty of the proposed LDV speed measurement method. For practical use, the specific values of the corresponding uncertainties can be obtained according to the instruments used and the measurement results. An accurate uncertainty model is essential when conducting research on the velocimetry methods of Laser Doppler Velocimetry (LDV). The uncertainty model can help us understand the various sources of errors that may be encountered during the measurement process and evaluate the impact of these errors on the final measurement results, which helps to evaluate and optimize the performance metrics of the LDV system, such as the measurement range, resolution, and repeatability, and ensures that the system can provide reliable data under different conditions.

We conducted two experimental tests to assess the performance and practicality of the proposed axial multipoint LDV method. The first test was aimed at measuring the tangential velocity of a rotating disk, which allowed us to evaluate the accuracy of the test system. The second test was designed to measure the velocity of the water flow through a pipe, which helped us assess the performance of the test system in a real-world setting.

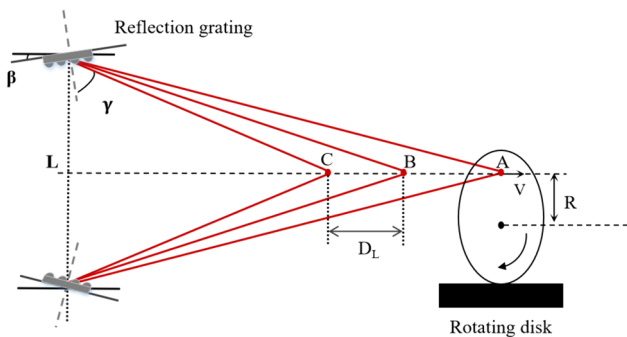
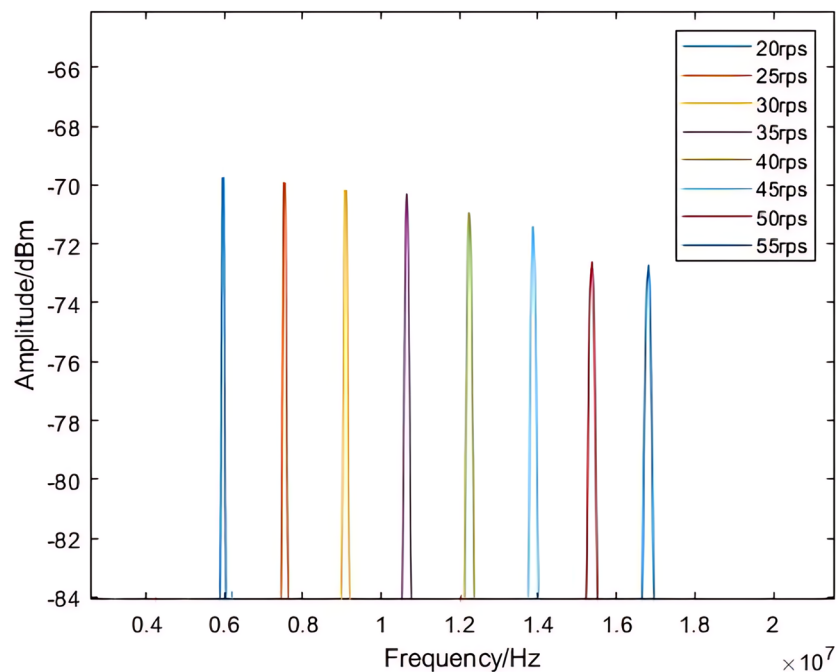


Fig. 2 Schematic diagram illustrating the measurement point locations concerning the rotational disk. Points A, B, and C correspond to measurement points obtained from zero-order, negative-first-order diffraction, and negative-second-order diffraction light, respectively. The distance between each measurement point and the center of rotation of the disk is denoted as R

3 Experiments and results

A single-frequency helium-neon (He-Ne) laser (Thorlabs, HNL100L) with a power of 10 mW and a wavelength of 632.8 nm was used as the light source. The laser output from the light source was divided into two paths by a 50/50 beam splitter. Each laser path was diffracted by a 600 lines/mm reflective grating (Edmund Optics, #15-763) to produce three levels of diffracted light, namely, zero, negative one, and negative two levels of light. Two diffracted light paths of the same magnitude intersect to form independent measurement points (A, B, C, shown in Fig. 2), and the distances between the measurement points are 96.8 mm and 30.8 mm, respectively. In this study, we measured the measured volumes of three measurement bodies A, B and C. The measured volume at point A has a thickness $\bar{d}_{0v}=0.22433$ mm and a length $2\bar{a}_0=1.154$ mm. The measured volume at point B has a thickness $\bar{d}_{1v}=0.34718$ mm and a length $2\bar{a}_1=0.72878$ mm. The measured volume at point C has a thickness $\bar{d}_{2v}=0.38476$ mm and a length $2\bar{a}_2=0.50864$ mm. The target is placed at each of the three measurement points, and the scattered light from the target is converged by a combination lens with a focal length of 75 mm and a lens with a focal length of 50 mm and is received by the photodetector (Thorlabs, Inc., APD430A2). The interference signals received by the APD were recorded and displayed by a digital oscilloscope (Rohde and Schwarz, RTB2002).

Fig. 3 Spectrogram of the Point A measuring body at different speeds



3.1 Rotating disk speed verification experiment

The disk is successively placed at measurement points A, B, and C, and its Doppler spectrum at different rotational speeds is recorded. The disk's rotational speed is monitored by a built-in counter and manually adjusted to 8 gears ranging from 20 to 55 rps, with a 5 rps increment. The rotational frequency drift of the selection disk used is $<0.5\%$. For each rotational speed of the disk, measure the Doppler spectrum 10 times. The distance between the measuring point and the center of rotation of the disc $R = 39.5$ mm. Figure 3 illustrates the measurement results of the Doppler spectrum at point A as a function of rotational speed. Due to the low signal-to-noise ratio of the raw interference signal captured by the oscilloscope, we used the wavelet-based denoising threshold algorithm the sliding average filtering algorithm for noise reduction, and the short-time discrete Fourier transform (STFT) for spectral analysis. At different rotational speeds, the Doppler frequency rises with the increase in rotational speed, and the signal amplitude is steady. The spectra are separated from each other without overlapping and have a single peak. At high rotational speeds, some spectra will show a slight broadening, which may lead to errors in peak extraction. However, these errors can be minimized by extracting the peaks several times and averaging them, while ensuring single-peakability. The spectral variations of the other measurement points are consistent with point A and are not shown here.

Figure 4 illustrates the velocity measurement results at different positions and under various rotational speeds. The results of subplots (a), (b), and (c) of Fig. 4 show that the

measured values of all measurement points increase linearly with increasing rotational speed, which indicates that the system has the ability to measure the axial velocity distribution. For comparative analysis, the velocity measurements at the three measurement points were compared with the theoretical values of the disk's rotational speed ($v = 2R\pi f$, R is the distance between the center of the measuring body and the center of the disc, and f is the rotation frequency of the rotating disk.). Within the range of rotational speeds, the average error values between the measured values and theoretical values at points A, B, and C are 0.2482 m/s, -0.2548 m/s, and -0.3088 m/s, respectively, with directional relative error (DRE) of 2.80%, -3.21% , and -3.35% . With the increase of rotational speed, the relative error has no obvious upward or downward trend, and the error at some points shows small fluctuations, which may be caused by slight changes in experimental conditions or measurement noise, such as rotational speed pulsation, environmental instability, and other factors. Overall, the measured and theoretical values of rotational speeds are in good agreement at different axial positions, and the error levels are comparable to the results of similar studies [3, 25–27]. For the comparison of the measurement results at different positions in the axial direction, it can be found that the measurement results at point A have the smallest relative error. This is because point A, as the target with the farthest measurement distance, has the smallest angle between the two beams of light, which

reduces the error caused by the detector aperture size and improves the accuracy of the measurement results [28].

3.2 Experiment on the measurement of water velocity

Flow velocity in the circulating water tank pipeline was measured using a constructed laser Doppler velocimetry system, and the schematic diagram of the experimental setup is shown in Fig. 5. The circulating water tank used (Beijing Changliu Company, Lx-1000) has a circulation flow range of 0–45 L/min, with the experimental water temperature controlled at 21 ± 1 °C. To simulate real-world applications, a transparent quartz square pipe measuring $8 \times 8 \times 60$ mm³ was fabricated as the measurement section. Apart from the measurement section, all the circulating water pipes have an outer diameter of 10 mm and an inner diameter of 9 mm. Downstream of the measurement section, a standard electronic flowmeter (ZMB Company, ZS-WL) with a precision of 2% was connected to the pipeline. The flow meter used can display both instantaneous and total flow rates, and the basic principle of measurement is to determine the volume flow rate of a fluid by measuring the number of times the fluid drives a gear to rotate. At the start of the experiment, the circulating water tank is activated, and testing commences once the flowmeter's instantaneous flow reading stabilizes at a fixed value. Following the conclusion of the test, the corresponding velocity is obtained based on the flowmeter's flow

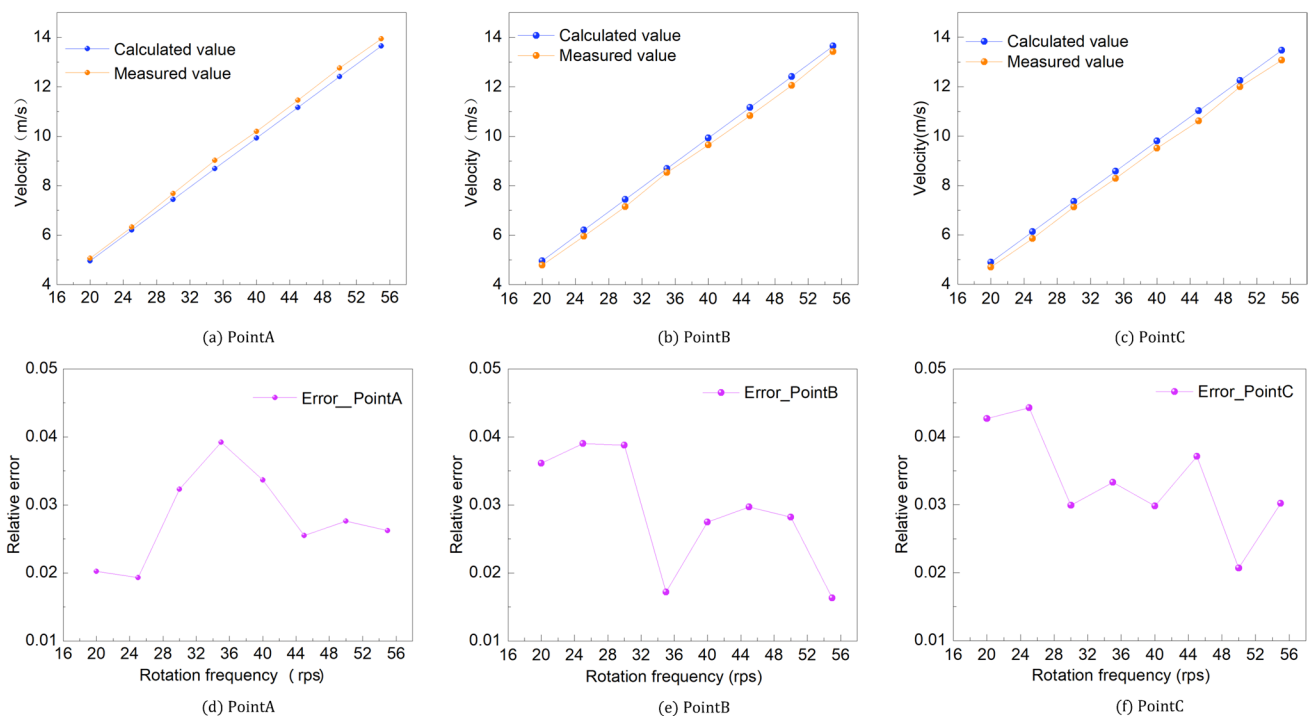


Fig. 4 Comparison of the measured and calculated values of disc speed at points A, B, and C

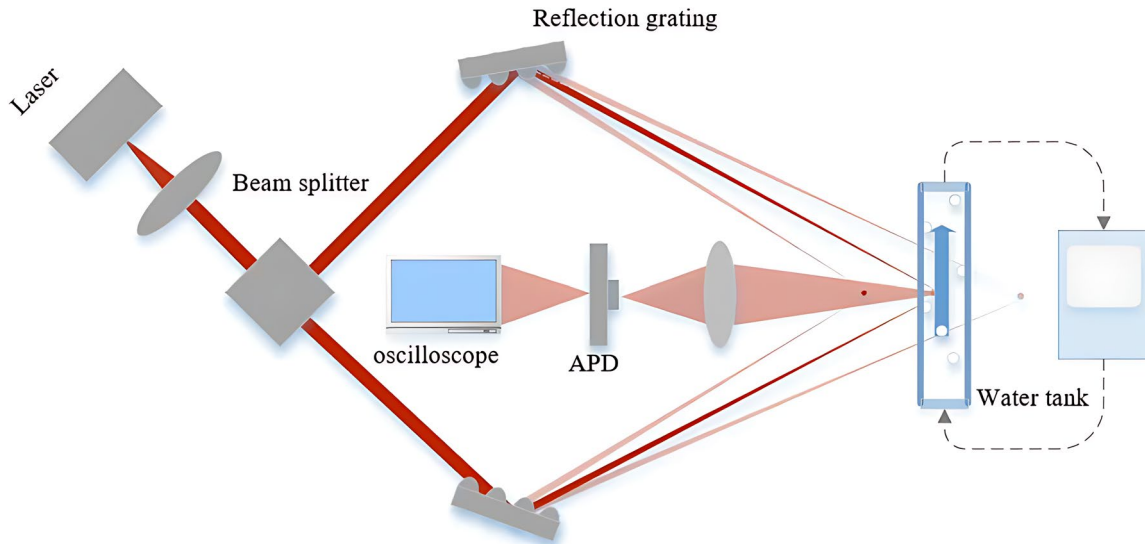


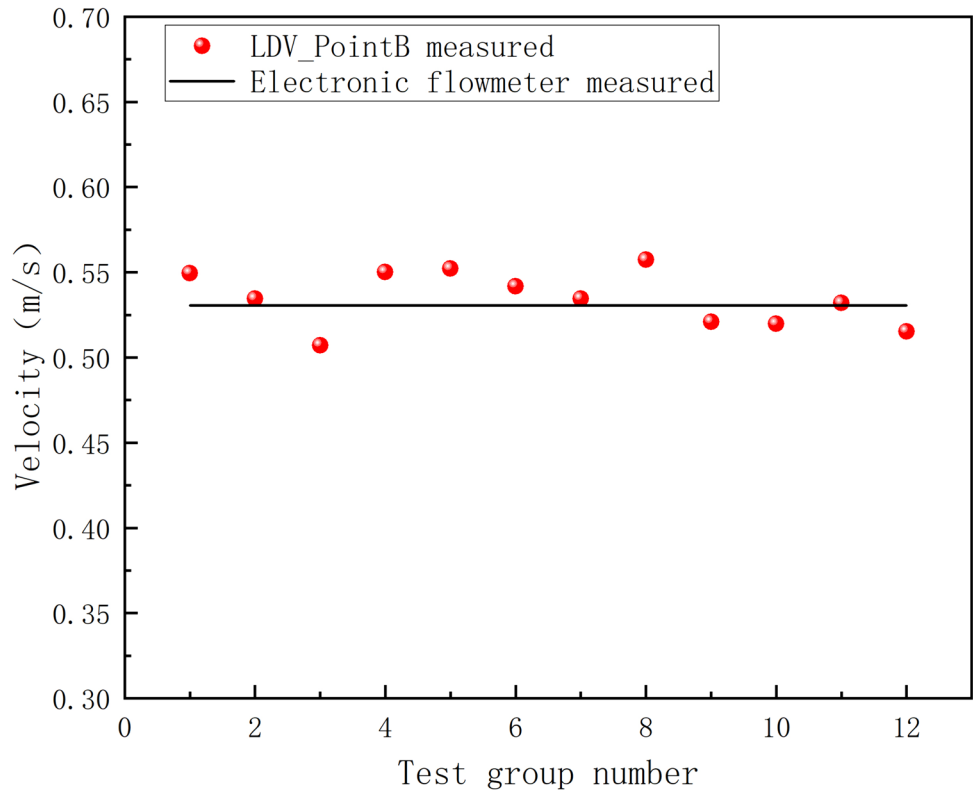
Fig. 5 Schematic diagram of liquid flow rate measurement experiment

readings. The flow rate measurement value of the standard flowmeter serves as a reference for the LDV. In the circulation system, water flows sequentially from the outlet of the water tank through the pipeline, transparent quartz square pipe, and the standard electronic flowmeter, before returning to the tank, forming a complete closed-loop flow. Prior to the measurement, the center of the square pipe was marked

with a marker pen on the upper surface and on the incident side with a positioning accuracy of approximately ± 0.5 mm. The measurement section is placed in the optical path of the constructed LDV, and negative first-order diffraction light is used for velocity measurement.

The average flow rate of the electronic flowmeter is recorded over one minute. At the same time, 12

Fig. 6 Comparison of the measured liquid velocity at measurement point **B** with that of a standard electronic flow meter



measurements were made with the LDV. The LDV measurements were compared with those of the standard electronic flowmeter and the results are shown in Fig. 6. The average velocity of the water flow measured by the electronic flowmeter was 0.5305 m/s. The maximum, minimum, and average values of the 12 LDV measurements were 0.5573 m/s, 0.5072 m/s, and 0.5346 m/s, respectively, with a standard deviation of 0.0162. The relative error of the average flow velocity measured by the LDV to the electronic flowmeter was 0.77%. The water velocity measured by the LDV system shows some fluctuation, which is affected by several factors. First, the LDV has a high temporal resolution and can measure instantaneous velocities, whereas the fluctuations reflect the possibility of unstable flow rates in the water tank pipe, which is a characteristic that cannot be captured by an electronic flowmeter. Secondly, the fluctuations also reflect the effects of inaccuracies in the measurement process, mainly in measurement inaccuracies and imperfections in the optical components as well as inaccuracies in Doppler shift peak extraction. By gaining a deeper understanding of these influences, we can comprehensively evaluate and improve the performance of measuring LDVs.

4 Conclusion

This paper presents a raster-guided axial multipoint laser Doppler velocimetry method, fully leveraging the advantages of the dual-beam laser Doppler velocimetry mode. By utilizing the multi-level diffraction of the reflective grating, multiple measurement points distributed along the axial direction are constructed, enabling velocity distribution measurement along the axis. A three-channel LDV testing system was constructed, successfully validating the experimental measurement of axial velocity distribution, with a maximum relative error not exceeding 4%. Comparing LDV measurements with those of a standard electronic flowmeter for pipe flow velocity, the relative error between the two was 0.77%. Future research will focus on optimizing the diffraction efficiency of the grating, improving signal processing, and considering the integration of spatial encoding techniques to achieve synchronous multipoint velocity measurement, thereby fully realizing the potential of multipoint LDV methods and advancing their application in fields such as fluid dynamics.

Author contribution Yu. Q.: Conceptualization, methodology, software, investigation, formal analysis, Writing—original draft; Liu. B.: conceptualization, data curation, writing—original Draft; Cong. Z.: visualization, investigation; Liu. Z.: resources, supervision; Zhang.X.: software, validation; Qu. L.: Visualization; Men. S. (Corresponding

Author): conceptualization, funding acquisition, resources, supervision, writing—review and editing.

Funding Project supported by the Natural Science Foundation of Shandong Province (Grant No. ZR2022DKX001), and the Taishan Scholars Project of Shandong Province (Grant No. tsqn201909007).

Data availability The data that support the findings of this study are available on request from the corresponding author, [MEN], upon reasonable request.

Code availability Not applicable.

Declarations

Conflict of interest (Check journal-specific guidelines for which heading to use). The authors have no competing interests to declare that are relevant to the content of this article.

Consent for publication This paper has not been published in other journals and has not been submitted to other journals at the same time to ensure the originality and independence of this paper. The authors of this paper agree to handle the paper in accordance with the normal paper publication process.

Ethics approval and consent to participate. Not applicable.

References

1. W.K. George, The laser-Doppler velocimeter and its application to the measurement of turbulence. *J. Fluid Mech.* **60**, 321–362 (2006)
2. V.V. Davydov, N.S. Myazin, S.E. Logunov, V.B. Fadeenko, A contactless method for testing inner walls of pipelines. *Russ J Nondestruct.* **54**, 213–221 (2018)
3. G. Zhang, B. Yu, J. Sun, L. Zhang, S. Zhen, Z. Cao, Deep-sea in-situ laser Doppler velocity measurement system. *Acta. Phys. Sin-Ch Ed.* **70**, 1000–3290 (2021)
4. M. Khalil, X.T. Rui, Q.C. Zha, H. Hendy, Investigation on spin-stabilized projectile trajectory observability based on flight stability. *Appl. Mech. Mater.* **530–531**, 175–180 (2014)
5. Y. Wang, J. Tan, R. Zhang, Measurement of Spinning projectile attitude based on polarization characteristics. *J. Ball.* **24**, 31–35 (2012)
6. H. Ishida, T. Andoh, S. Akiguchi, H. Shirakawa, D. Kobayashi, Y. Kuraishi, T. Hachiga, Blood flow velocity imaging of malignant melanoma by micro multipoint laser Doppler velocimetry. *Appl. Phys. Lett.* **97**, 333 (2010)
7. H.N. Lee, D.Y. Yan, C.Y. Huang, S.C. Chen, C.Y. Pan, J.H. Jeng, Y.K. Chen, F.H. Chuang, Laser Doppler for accurate diagnosis of Oehler's type III dens invaginatus: a case report. *Appl. Sci.-Basel.* (2021). <https://doi.org/10.3390/app11093848>
8. F.J. Wang, S. Krause, J. Hug, C. Rembe, A contactless laser Doppler strain sensor for fatigue testing with resonance-testing machine. *Sensors* (2021). <https://doi.org/10.3390/s21010319>
9. I.K. Tragazikis, D.A. Exarchos, P.T. Dalla, K. Dassios, T.E. Matikas, I.E. Psarobas, Elastodynamic response of three-dimensional phononic crystals using laser Doppler vibrometry. *J. Phys. D: Appl. Phys.* **52**, 285305 (2019)

10. C.T. Rodenbeck, J.B. Beun, Identifying the operation of a parked car's engine, transmission, and door using millimetre wave pulse Doppler radar. *Electron Lett.* **56**, 960 (2020)
11. M.A.A. Ismail, M. Schewe, C. Rembe, M. Mahmod, M. Kiehn, Traffic-induced vibration monitoring using laser vibrometry: preliminary experiments. *Remote Sens.* **14**, 6034 (2022)
12. E.B. Li, J. Xi, J.F. Chicharo, J.Q. Yao, D.Y. Yu, Multi-point laser Doppler velocimeter. *Opt. Commun.* **245**, 309–313 (2005)
13. C. Yang, M. Guo, H. Liu, K. Yan, Y.J. Xu, H. Miao, Y. Fu, A multi-point laser Doppler vibrometer with fiber-based configuration. *Rev Sci Instrum.* (2013). <https://doi.org/10.1063/1.4845335>
14. K. Maru, K. Kobayashi, Y. Fujii, Multi-point differential laser doppler velocimeter using arrayed waveguide gratings with small wavelength sensitivity. *Opt. Express* **18**, 301–308 (2010)
15. K. Maru, K. Fujimoto, Demonstration of two-point velocity measurement using diffraction grating elements for integrated multi-point differential laser Doppler velocimeter. *Optik* **125**, 1625–1628 (2014)
16. Y. Fu, M. Guo, P.B. Phua, Spatially encoded multibeam laser Doppler vibrometry using a single photodetector. *Opt. Lett.* **35**, 1356–1358 (2010)
17. T. Kyoden, S. Akiguchi, T. Tajiri, T. Andoh, N. Furuichi, Assessing the infinitely expanding intersection region for the development of large-scale multipoint laser Doppler velocimetry. *Flow Meas. Instrum* **70**, 101660 (2019)
18. H. Ishida, D. Kobayashi, H. Shirakawa, T. Andoh, S. Akiguchi, T. Wakisaka, M. Ishizuka, T. Hachiga, Note: Reflection-type micro multipoint laser Doppler velocimeter for measuring velocity distributions in blood vessels. *Rev. Sci. Instrum.* **82**, 25 (2011)
19. H. Lshida, H. Shirakawa, T. Andoh, S. Akiguchi, D. Kobayashi, K. Ueyama, Y. Kuraishi, T. Hachiga, Three-dimensional imaging techniques for microvessels using multipoint laser Doppler velocimeter. *J. Appl. Phys.* **106**, 017002 (2009)
20. K. Maru, Axial scanning laser Doppler velocimeter using wavelength change without moving mechanism in sensor probe. *Opt. Express* **19**, 5960–5969 (2011)
21. K. Maru, K. Watanabe, Cross-sectional laser Doppler velocimetry with nonmechanical scanning of points spatially encoded by multichannel serrodyne frequency shifting. *Opt. Lett.* **39**, 135–138 (2014)
22. S.N.A.B. Abd Ghafar, H. Yamaji, K. Maru, Laser Doppler velocimetry for three-dimensional distribution measurement of the velocity component by combining two-dimensional spatial encoding and non-mechanical scanning. *Appl Optics.* **61**, 5640–5645 (2022)
23. C.P. Wang, Laser Doppler velocimetry. *J Quant Spectrosc Ra.* **40**, 309–319 (1988)
24. BIPM, IEC, IFCC, ILAC, Biotechniques, O.J.: Evaluation of measurement data—Guide to the expression of uncertainty in measurement. (2008).
25. Li, X.: Research on laser velocimetry technology under strong infrared radiation background. *Proc. SPIE (USA)*. 125540W (125511 pp.)-125540W (125511 pp.) (2023).
26. L. Ma, Experimental verification of dual beam laser Doppler speed measurement system. *Appl Laser.* **43**, 116–119 (2023)
27. S. Kato, T. Ichikawa, H. Ito, M. Matsuda, N. Takahashi, Multipoint sensing laser Doppler velocimetry based on laser diode frequency modulation. *OFS* **1**, 606–609 (1996)
28. J. Zhou, Q. Feng, S. Ma, R. Song, G. Wei, X. Long, Error analysis of reference-beam laser Doppler velocimeter. *High Power Laser Part. Beams* **22**, 2581–2587 (2010)

Publisher's Note Springer Nature remains neutral with regard to jurisdictional claims in published maps and institutional affiliations.

Springer Nature or its licensor (e.g. a society or other partner) holds exclusive rights to this article under a publishing agreement with the author(s) or other rightsholder(s); author self-archiving of the accepted manuscript version of this article is solely governed by the terms of such publishing agreement and applicable law.